Holocurtains: Programming Light Curtains via Binary Holography

Dorian Chan, Srinivasa G. Narasimhan, and Matthew O'Toole
Carnegie Mellon University, Pittsburgh, PA 15213, USA
[dychan, srinivas, motoole2]@andrew.cmu.edu

Abstract

Light curtain systems are designed for detecting the presence of objects within a user-defined 3D region of space, which has many applications across vision and robotics. However, the shape of light curtains have so far been limited to ruled surfaces, i.e.*, surfaces composed of straight lines. In this work, we propose Holocurtains: a light-efficient approach to producing light curtains of arbitrary shape. The key idea is to synchronize a rolling-shutter camera with a 2D holographic projector, which steers (rather than block) light to generate bright structured light patterns. Our prototype projector uses a binary digital micromirror device (DMD) to generate the holographic interference patterns at high speeds. Our system produces 3D light curtains that cannot be achieved with traditional light curtain setups and thus enables all-new applications, including the ability to simultaneously capture multiple light curtains in a single frame, detect subtle changes in scene geometry, and transform any 3D surface into an optical touch interface.*

1. Introduction

A light curtain is an optical barrier that detects the presence or absence of objects within regions of 3D space [2]. For example, light curtains are used in elevators and garage doors, in order to keep doors open when a person or object is in the doorway. Safety light curtains also are used in environments containing hazardous equipment (*e.g.*, machine tools, robotic arms) to protect personnel from injury, by automatically turning off dangerous machinery whenever a curtain is breached.

These light curtains involve two key components: emitters and receivers. Traditional light curtains position an emitter to directly illuminate a receiver through direct line of sight. If an obstacle blocks the light traveling from the emitter to the receiver, the drop in the detected light signal triggers an event. While extremely reliable and simple devices, light curtains must be physically configured for their specific environments, which is a laborious process.

Wang *et al*. [35] recently proposed a programmable approach to generate light curtains through triangulation. A scene is illuminated with a laser line, and the response is measured with a line scan camera [35] or a rolling-shutter camera [5]. The intersection of the illumination and sensing planes produces a 3D line (see Fig. 2(a)). If an object touches this line, light from the source reflects off the object and reaches the camera—triggering an event. Rapidly changing the position of the illumination and sensing planes (*e.g.*, with mirror galvanometers) creates ruled surfaces, *i.e.*, surfaces defined by unions of straight lines. Triangulation light curtains offer several benefits, including the ability to program the shape in real time and operate under strong ambient light, which can potentially be leveraged for new safety applications including assisted or autonomous navi-

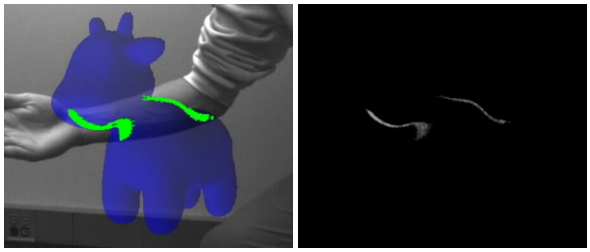

(a) An arm passes through a toy cow-shaped light curtain

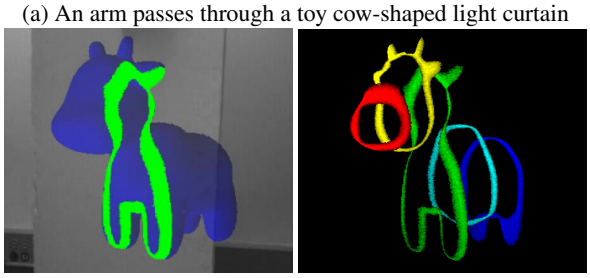

(b) A foam board sweeps through the light curtain

Figure 1. Our Holocurtain system turns a user-defined volume or surface (*e.g.*, a toy cow) into a 3D light curtain. **(a)** An arm passes through the light curtain. In the left image, blue pixels represent the light curtain and green pixels highlight areas intersecting the light curtain. The right image represents the raw data from the system used to detect the intersections. **(b)** The left image shows a foam board moving through the light curtain. The right image is a composition of raw measurements captured at different instances in time, where the colors represent different frames.

gation through unknown environments [3, 4, 26].

Despite these advantages, a key limitation is that these light curtains have been fundamentally restricted to being ruled surfaces. Moreover, prior systems offer only one degree of freedom over the positions of the laser line and scan line, limiting triangulation light curtains to an even smaller subset of ruled surfaces. Current prototype systems are only designed to produce either predominantly vertical curtains [5, 35] or horizontal curtains [32, 34].

In this work, we remove the constraints on the shape of light curtains by exploring a novel approach to structured illumination. Specifically, we replace the laser line with a projector capable of generating arbitrary illumination patterns by redistributing light at high speeds (up to 10 kHz). We propose using 2D computer-generated holography to produce structured light patterns, which has the advantage of having much higher light efficiency than conventional projectors. When synchronized with a rolling-shutter camera, our system is capable of generating light curtains of arbitrary shape, as illustrated in Fig. 2(b). Moreover, we demonstrate the ability to multiplex multiple light curtains into a single measurement. We leverage these new capabilities for a number of new applications, including optical disturbance detection and 3D optical touch sensing.

The contributions of our work include the following:

- a holographic light curtain technique, capable of generating curtains of arbitrary shape;
- a spatial multiplexing strategy to capture the response from multiple curtains in a single image; and
- an approach to structured lighting that involves high-speed and light-efficient 2D holography.

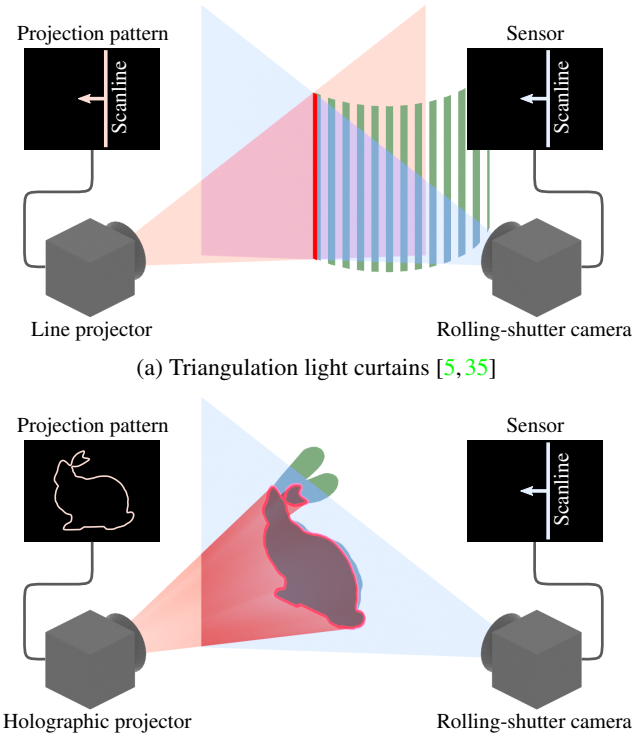

(a) Triangulation light curtains [5, 35]

(b) Holocurtains **[ours]**

Figure 2. Illustration of light curtain systems. **(a)** A triangulation light curtain combines a laser line with either a 1D line sensor [35] or a rolling-shutter camera [5]. The light curtain (green) is formed at the intersection of the illumination plane (red) and sensing plane (blue), which are synchronously scanned together to form a ruled surface. **(b)** We propose using holographic projector that steers light to select regions of the scene at high speeds. The light curtain of a bunny is formed by synchronizing projection patterns (cross-sections of the bunny) with the rolling-shutter sensor.

2. Related Work

Light curtains require structured lighting, a process that involves projecting light patterns into a scene. Structured lighting is also used across many other vision tasks, including 3D scanning [14], decomposing scene appearance [19], and light transport probing [20–22]. As a result, there are many options to generating light patterns as outlined in Tab. 1, each one with its own advantages and disadvantages.

Many consumer devices make use of static structured lighting patterns. For example, iPhones and iPads use dot projectors to implement their Face ID feature. These dot projectors consist of arrays of VCSELs (vertical cavity surface emitting lasers), where every VCSEL illuminates a spot in the scene. Another example is laser line levels, tools used in the construction industry that produce horizontal or vertical laser lines across a surface. As previously discussed, conventional light curtains also use emitters to project light beams towards receivers. Although simple, reliable, and compact, these lighting solutions are not programmable.

To add programmability, mirror galvanometers can be used to steer laser beams or lines across the scene. For instance, this solution is used by commercial 3D scanners [1] and triangulation light curtains [5, 35]. MEMS mirrors, used in certain laser projectors, can also be used to raster scan a scene with a laser beam at fast rates [15], a solution adopted by slope-disparity gating [32, 34] and Episcan3D [20]. However, these solutions are limited to generating structured light patterns through continuous scans.

The most common and flexible form of structured lighting involves conventional LCD or DLP projectors. A significant amount of work exists in optimizing the structured light patterns for these projectors. For example, this includes multiplexing schemes to boost SNR [28], or strategies to more efficiently capture 3D shape [13, 27]. Unfortunately, off-the-shelf projectors can be extremely light inefficient. For example, to project a thin line into a scene, the light from all other projector pixels must be blocked.

To strike a balance between these different structured

Technology	Light Efficiency	Pattern Rate	Programmability	References
Static Pattern	High	N/A	None	[2]
Galvo Mirror	High	≈ 250 Hz	Arbitrary Scan Pattern	[5, 35]
MEMS Mirror	High	≥ 10 kHz	Lissajous Pattern	[20, 32, 34]
LCD Projector	Low	≈ 60 Hz	Arbitrary Pattern	[22]
DLP Projector	Low	≥ 10 kHz	Binary Pattern	[20]
Binary Holography	High	≥ 10 kHz	Arbitrary Pattern	Ours

Table 1. Comparison of different structured lighting solutions. The right-most column references works that apply the corresponding technology to generate different types of light curtains (which includes disparity gating [20, 32, 34] and optical z-keying [22]).

light solutions, Gupta *et al*. [14] explored the concept of light redistribution in the context of structured light 3D scanning. Given a fixed light budget, the idea was to redistribute the available light to form structured light patterns. This solution offered the ability to capture the 3D shape of objects under strong sunlight. This idea was further explored in the context of light transport probing [20], to produce energy-efficient imaging solutions for a variety of problems (3D reconstruction under sunlight, direct and indirect separation, and imaging through scattering media). However, their prototype systems were once again constrained to certain types of projector patterns (*i.e*., they involved spinning polygonal mirrors and raster-scanning laser projectors). In this work, we explore light redistribution in the context of light curtains, and develop a holographic projector capable of arbitrarily redistributing light at high speeds. As a new approach to structured lighting, we also believe this solution may be influential for other vision problems (*e.g*., structured light 3D scanning and light transport probing).

3. Generating an Arbitrary Light Curtain

The objective of a light curtain is to detect if an object touches a user-defined virtual surface G. This can be done with a camera and projector, by following three simple steps: expose a single camera pixel on the sensor, computationally intersect the camera ray with virtual surface G, and project a pattern that selectively illuminates the intersection. Although this procedure creates the desired light curtain, this naive solution would need to be repeated for every camera pixel individually—a time consuming endeavor.

Instead, one can start by simultaneously exposing an entire row (or column) of pixels to produce a planar viewing frustum, or sensing plane (see Fig. 2). The next step is to compute the intersection between this plane and the virtual surface G. Finally, the projector can then selectively illuminate the intersected regions.[1] This process would be repeated for every row of pixels on the sensor.

To produce light curtains of arbitrary shape, we desire three key properties from the projector: high light efficiency, speed, and programmability. For example, LCD and DLP projectors are highly programmable, capable of displaying any structured light pattern given as input. However, these projectors are also very light inefficient; when given a sparse pattern as input, most of the light emitted by these projectors is blocked. Using such projectors limits the working range and reliability of a light curtain system. Prior light curtain solutions therefore opt to use either a galvo mirror system [5, 35] or MEMS mirror [20, 32, 34] to scan a laser line across the scene. However, because these prior works could only project line patterns, the shape of G was constrained to being a ruled surface. As a result, there are no off-the-shelf structured lighting solutions that meet all the criteria necessary to produce arbitrary light curtains.

4. Computer-Generated Binary Holography

To address the criteria required for generating arbitrary light curtains, we propose using computer-generated binary holography [7, 8] to form structured light patterns.

A holographic projector uses the principles of wave optics to form interference patterns that match a target projection pattern. In 1966, Brown and Lohmann [7, 8] reported the first computer-generated holograms, created by printing binary patterns with a computer-controlled mechanical plotter. Since then, a number of papers have shown that binary DMDs (digital micromirror devices, used in DLP projectors) can be utilized holographically for a variety of applications, including optical tweezers [30, 31], beam forming [9, 18, 33], microscopy [10], nanomanufacturing [11], aberration correction [25] and 3D displays [16]. However, to our knowledge, our work is first to utilize holography as a structured lighting solution for computer vision problems.

4.1. Fourier-Transform Holography

Consider the Fourier-transform holography setup shown in Fig. 3. A collimated beam of light illuminates a spatial light modulator (SLM) positioned at the Fourier plane (*i.e*., at the front focal plane of lens 2). The SLM modulates the wavefront's amplitude or phase, and the reflected light is focused by a lens to form an interference pattern at the image

[1] This step assumes that the sensing plane is not an epipolar plane of the projector-camera system.

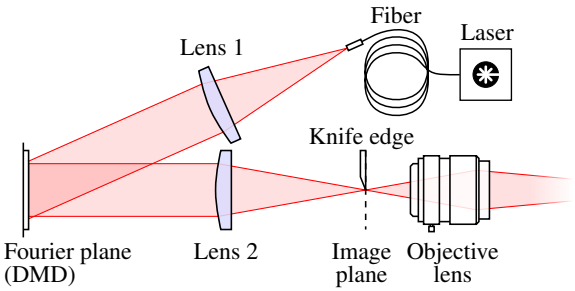

(a) Illustration of projector optics

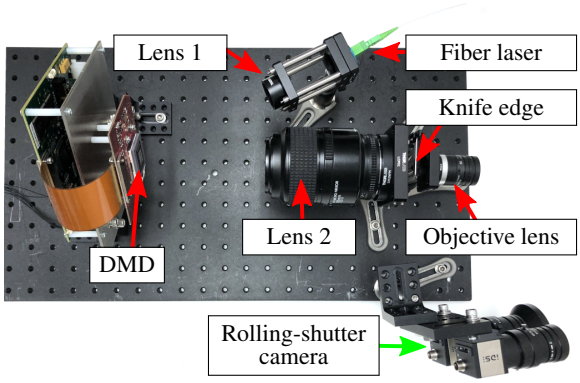

(b) Photo of light curtain setup

Figure 3. Overview of prototype holographic projector. **(a)** Illustration of setup. The light from a 530 nm fiber-pigtailed laser is collimated by a lens, and illuminates a DMD (digital micromirror device) at a 24° angle. The DMD selectively reflects light back through a second lens, which forms a holographic image at the image plane. Since this image is conjugate-symmetric, we position a knife-edge aperture to block half of the image, along with the bright DC component. An objective lens projects the resulting image into the scene. **(b)** Photo of the prototype setup, which includes both the projector optics and the rolling-shutter camera used for generating light curtains.

plane (*i.e.*, at the back focal plane of lens 2). This image formation model for the wavefront $U(s,t)$ at the image plane can be expressed as follows:

$$U(s,t) = \mathcal{F}\{u(x,y) \cdot a(x,y)\}(s,t), \tag{1}$$

where $u(x,y)$ is the pattern displayed on the SLM, $a(x,y)$ represents optical aberrations associated with imperfections with the SLM, and $\mathcal{F}\{\cdot\}$ is the Fourier transform operator that models wavefront propagation from the Fourier plane to the image plane. Note that the intensity of a wavefront, which is the signal measured by a camera, is given by its squared magnitude (*e.g.*, $|U(s,t)|^2$).

For the SLM, we use a DMD, a device composed of an array of mirrors that have $\pm 12°$ tilt angle states, to provide binary amplitude modulation of the wavefront. Every mirror can be turned on (1) or off (0). Although phase SLMs are often used in holography for their superior reconstruction results, the pattern rate of phase SLMs is typically 60 Hz. In contrast, DMDs offer pattern rates up to 30 kHz.

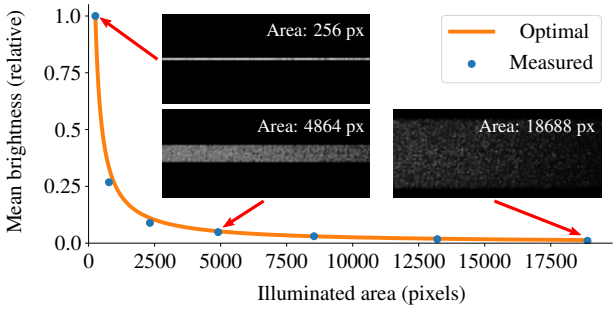

Figure 4. Our holographic projector is light redistributive. To verify this, we projected lines of different thicknesses onto a flat diffuse white surface, and measured the average brightness of each line using an exposure stack to form an HDR image. The pattern brightens as the illuminated area decreases. We also plot an estimate of the optimal light redistribution curve, which we computed by taking the sum of the brightnesses of the thinnest line, and normalizing that value by the range of areas. Our measurements closely match the optimal light redistribution curve, where brightness is inversely proportional to illuminated area.

There are two notable characteristics of holograms created with a DMD. For simplicity, let's assume that optical aberrations are negligible (*i.e.*, $a(x,y) = 1$). The Fourier transform of any binary pattern is conjugate symmetric and has a strong DC component (related to the number of pixels turned on). We therefore use a knife edge positioned at the image plane to block both the DC and the symmetric copy of the hologram, and use an objective lens to project the remainder of the image into the scene. The objective lens scales the pattern to match the camera's field of view.

An important property of a holographic projector is that it reallocates light from dark regions towards light parts of the image. This is exemplified in Fig. 4, which shows holograms of lines with different thicknesses. The intensity of the line is inversely proportional to the thickness of the line. Note that at least 87.5% of the light is still wasted, as only half of the DMD pixels are typically turned on and the knife edge blocks half of the image as well as the DC spot; we measured a loss of 92% in our setup. While this may not be as light efficient as line projection solutions, our system has the added benefit of being able to generate arbitrary patterns. In addition, many of the contributing factors could be avoided by using a fast phase-only SLM [6].

4.2. Modified Gerchberg-Saxton Algorithm

In 2D computer-generated holography, the objective is to compute a pattern $u(x,y)$ that produces a target image $I(s,t) = |U(s,t)|^2$. To achieve this, we use a modified

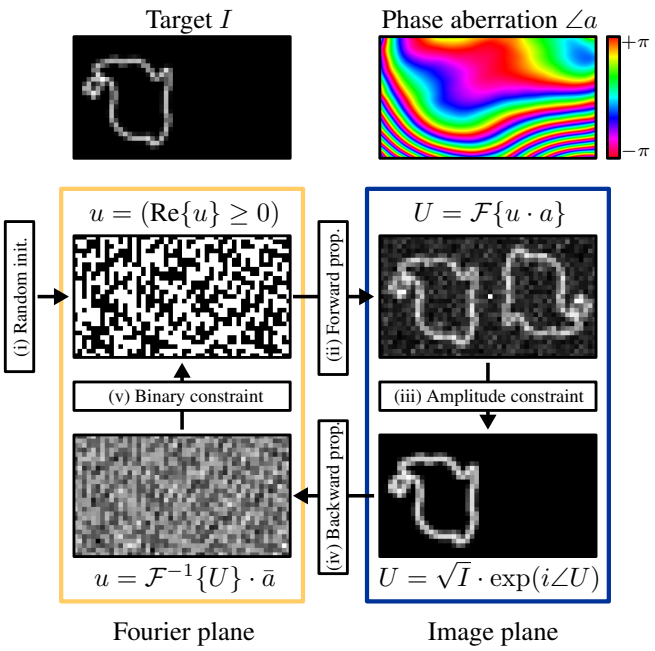

Figure 5. Flowchart for our modified Gerchberg-Saxton (GS) algorithm. Given a target image I and complex-valued phase aberration image a, the objective is to find a binary pattern that can be displayed on a DMD to reproduce the target image. GS starts by **(i)** initially starting with a random binary pattern, **(ii)** propagating the wavefront from the Fourier plane to the image plane, **(iii)** replacing the wavefront's amplitude with $\sqrt{I}$, **(iv)** propagating the wavefront from the image plane to the Fourier plane, and **(v)** binarizing the result. The GS algorithm quickly converges after a few iterations. An important attribute of our GS algorithm is that it accounts for large phase aberrations created by the DMD, producing sharper target image reconstructions as a result.

Gerchberg-Saxton (GS) algorithm [12], similar to past work in binary holography [17, 24, 30]. The algorithm alternates between enforcing a constraint on the hologram's intensity at the image plane, and enforcing the binary constraint on the DMD pattern at the Fourier plane.

After initializing the DMD pattern $u(x, y)$ with random binary values, the algorithm iteratively performs four simple operations to compute the hologram, as highlighted in Fig. 5. First, we use Eq. (1) to simulate the propagation of the wavefront from the Fourier plane to the image plane. This involves performing an element-wise multiplication with a pre-computed phase pattern $a(x, y)$ and computing the Fourier transform of the result, producing a conjugate-symmetric wavefront $U(s, t)$. Second, we keep the phase $\angle U(s, t)$ of this wavefront, but replace its amplitude to match the target intensity image. Third, we invert the propagation operator by using an inverse Fourier transform and performing an element-wise multiplication with the complex conjugate of the phase pattern $a(x, y)$. And fourth, we binarize the result, by setting all values with positive real components to 1 and setting all other values to 0. The GS algorithm repeats these four steps until convergence, which typically requires only a few iterations.

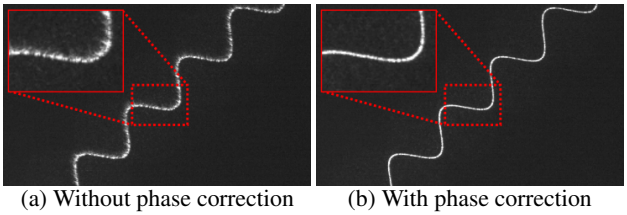

(a) Without phase correction (b) With phase correction

Figure 6. Effect of calibrating for the phase distortion of the binary DMD. **(a)** A sinusoid pattern generated without taking into account the phase. **(b)** A sinusoid that corrects for the phase as part of the GS algorithm. Calibrating for the distortion caused by phase aberrations at the Fourier plane creates a sharper curve.

4.3. Calibrating the DMD

In practice, the light reflecting off of the DMD is affected by aberrations. We attribute the most severe aberrations to the non-planarity of the DMD's surface, which can be characterized by a spatially-varying phase pattern $a(x, y)$. Ignoring these aberrations results in blurry holograms, as shown in Fig. 6(a). We therefore pre-compute the phase aberration image $a(x, y)$ and use our GS algorithm to produce sharper holographic images, as shown in Fig. 6(b).

To calibrate for this distortion, prior works divided the DMD into blocks of pixels and turned on pairs of blocks at the same time to produce interference patterns [30, 33]. By measuring these interference patterns, one can compute the relative phase between the two blocks of pixels.

We instead opt for a simpler approach that does not rely on interfering pairs of DMD blocks. The first step is to display a block of pixels on the DMD, where pixels within this block are randomly turned on or off. This forms a random interference pattern, which we image with a camera. Next, we slide this block to different DMD regions, and record the corresponding interference patterns. If the phase pattern varies linearly across a block, this shifts the observed interference pattern. We measure the shifts by performing zero-normalized cross-correlation between every measurement and a reference interference pattern, and compute the corresponding gradients on the phase pattern. Finally, we solve a large linear system to compute the spatially-varying phase values from these phase gradients, which is equivalent to solving a Poisson equation [29]. We describe this approach in more technical detail in the supplement.

The phase for our recovered aberration image is shown in Fig. 5. Our calculations indicate that the surface of our DMD varies by approximately $7.3\lambda \approx 3.87\,\mu\text{m}$, where $\lambda = 530\,\text{nm}$ is the wavelength of our light source.

5. Hardware Setup

We show an image of our hardware setup in Fig. 3(b). For our laser source, we use a Coherent Sapphire LPX 530-300 Laser, which emits $530\,\mathrm{nm}$ light anywhere from $10\,\mathrm{mW}$ to $330\,\mathrm{mW}$. We use $300\,\mathrm{mW}$ for our experiments. The laser light is collimated using lens 1, a $75\,\mathrm{mm}$ achromatic doublet (Thorlabs AC254-075-A-ML). A DLP Lightcrafter 6500 EVM from Texas Instruments controls the binary DMD, which has a resolution of 1920×1080, and operates up to $9523\,\mathrm{Hz}$; we use the Pycrafter 6500 library [25] to interface with the device. Lens 2 is a $105\,\mathrm{mm}$ $f/2.8$ DSLR lens (Nikon AF Micro-Nikkor) focused at infinity. We used a $9\,\mathrm{mm}$ $f/1.4$ lens (Fujinon HF9HA) for the objective lens. Our optics are angled to select the brightest mode that appears from the DMD and a knife edge at the image plane blocks the bright DC component and the conjugate-symmetric copy, as described in Sec. 4.

For the rolling-shutter camera, we used a UI-3240CP-NIR camera, fitted with a $8\,\mathrm{mm}$ $f/1.4$ lens and operated in $2\times$ binning mode for an image resolution of 640×512. We also mounted a $531\,\mathrm{nm}$ bandpass filter with a $10\,\mathrm{nm}$ FWHM to reject ambient light. To match the temporal resolutions of the DMD and the rolling-shutter camera, we ran the DMD at about $7575\,\mathrm{Hz}$ with a $40\,\mathrm{MHz}$ pixel clock at the camera for a final framerate of $28.64\,\mathrm{Hz}$, with 256 projector patterns per frame. We set the exposure of the camera to the pattern exposure time of the DMD. This camera was placed about $18\,\mathrm{cm}$ from the projector's center of projection. We describe more details of the calibration in the supplement.

We also added an additional UI-3240CP-NIR camera mounted with a $537\,\mathrm{nm}$ notch filter with a $162\,\mathrm{nm}$ FWHM to aid with visualization. For this camera, we used $2\times$ binning mode with a $6\,\mathrm{mm}$ $f/1.2$ lens.

6. Results

As we showed in Sec. 4, our setup allows us to generate arbitrary light curtains. To illustrate the new capabilities of our system, we demonstrate four different categories of tasks that are difficult or inefficient for other programmable light curtain setups.

Light Curtains of Arbitrary Shape. To start, we use our system to simultaneously generate both a flat and vertical light curtain in Fig. 7. Current prototype light curtain systems [5, 35] can only form one of the flat or vertical curtains, but not both at the same time. Our holographic projector system has no such limitations, and supports placing bounding boxes around objects.

We generate a three-dimensional light curtain in Fig. 1 of complex shape. In Fig. 8, we use our system to selectively image objects in a scene, such that the confidentiality of a sensitive document is preserved. In particular, such light curtains could be useful for robot safety applications. For example, Fig. 9 shows a form-fitting light curtain $5\,\mathrm{cm}$ off the body of a mannequin. A robot could use such a light curtain to detect whether it is too close to a person or object. For example, this could be used for assisted feeding, to aid those who cannot manage to feed themselves.

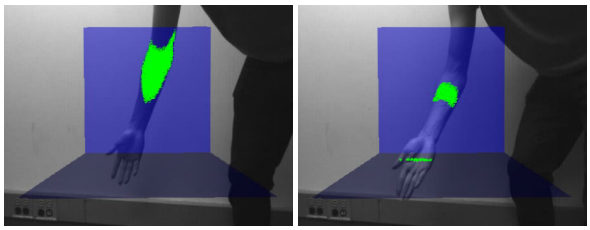

Figure 7. Our system can simultaneously form light curtains of different orientations. In this figure, we simultaneously place both a vertical and horizontal light curtain into the scene. Over the course of a single rolling-shutter exposure, our system is able to detect objects intersecting either of these curtains.

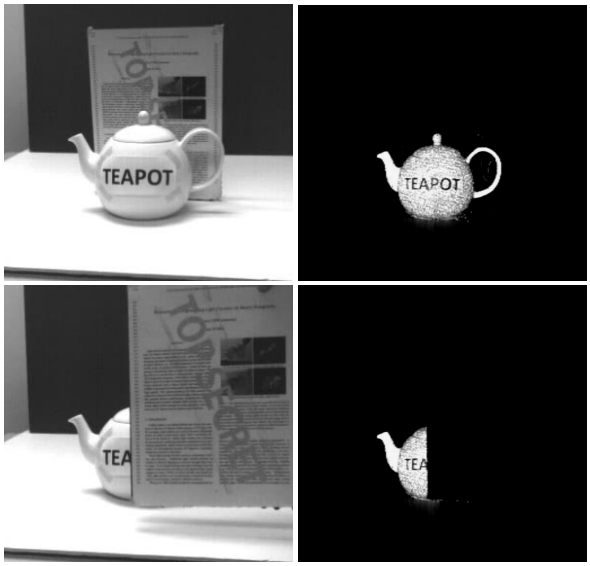

Figure 8. Similar to Ueda *et al*. [34], our system can selectively image user-specified 3D regions within the scene, like a teapot in this example. However, the advantage of our approach is that these regions can take on any 3D shape. The light from all objects not contained within this 3D region is optically filtered out, including the light reflecting off of a top secret document.

Disturbance Detection. A light curtain system can determine whether objects in a scene have been disturbed, by forming a tight light curtain over the surfaces of the scene. If no objects have been disturbed, our rolling-shutter camera records a bright image. In contrast, if objects have been moved, damaged, or dented, the measured intensity decreases in places where the object no longer lines up with the light curtain. Thus, we can extract a *disturbance map* by first imaging this light curtain when the scene is undisturbed, and subtracting the light curtain output after dis-

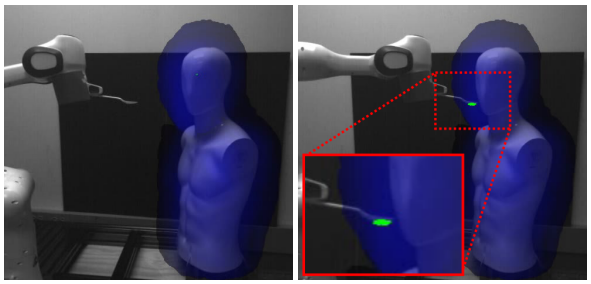

Figure 9. Our system can create form-fitting light curtains. Here, we create a light curtain 5 cm off the surface of a mannequin. Such a light curtain could be used in robot safety applications to detect if a robot gets too close to a person or delicate object. Feeding robots could also use these curtains as a cue for where to place a spoon, as shown above. Note that the visualization may be misleading - the handle of the spoon is in front, not behind the curtain.

turbance. In effect, this captures a difference image over a specific geometry of interest. We demonstrate an example of this disturbance detection in Fig. 11. If any objects are disturbed, the recorded images registers a significant, dense change in contrast to the low-intensity, sparse output of a difference image. This idea may have important implications in manufacturing; for example, if mounted over an assembly line, our device could inspect whether objects passing through have defects.

Multiple Simultaneous Light Curtains. We show that our system can simultaneously generate and separate multiple light curtains within a single rolling-shutter frame. This is done by interleaving the patterns associated with two (or more) target light curtains. We show an example of such a setup applied to a toy scene in Fig. 10.

To demonstrate why this might be useful, we show that the disturbance detection idea from the previous section can be combined with multiplexing to estimate the magnitude of a disturbance in Fig. 12. Our system projects two curtains: a thin curtain and a thick curtain. If the thick curtain receives signal while the thin curtain receives no signal, the disturbance must be small. However, if both curtains receive no signal, the disturbance much be large.

Three-Dimensional Touch Interface. We also demonstrate an optical three-dimensional touch interface in Fig. 13(a). We form a light curtain about 2 cm above some desired surface. When a person's finger interacts with this surface, the light curtain detects its location. While the setup given in Tsuji *et al*. [32] was limited to planar surfaces, our system can turn any arbitrary geometry into a virtual touch interface. In the space of augmented reality, detecting where a user interacts with a scene could be used as a new input for art or entertainment applications. For example, as shown in Fig. 13(b), our methodology can be used to turn any real-life object into a virtual drawing surface.

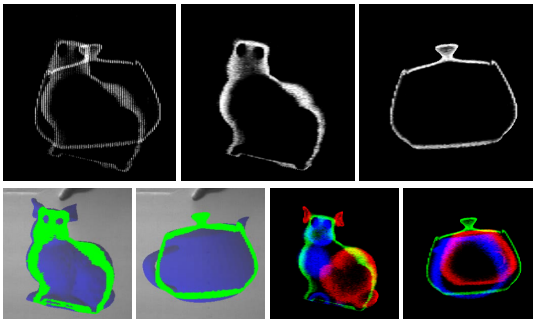

Figure 10. Our system can simultaneously capture multiple light curtains. **Row 1:** The demultiplexing process. In the leftmost raw image, even columns correspond to a bunny curtain while odd columns correspond to a teapot curtain. The separated curtains are shown in the middle and right images. **Row 2:** Sweeping a foam board through the curtains. Three positions of the board are represented by different colors in the two rightmost images.

7. Limitations

Two key limitations arise when using DMDs for 2D holography. First, binary control over the wavefront provides limited reconstruction quality. Artifacts manifest themselves in the form of speckle, which reduces the contrast of the generated pattern. Second, as previously described in Sec. 4.1, we lose at least 87.5% of light due to the binary nature of our holograms. These issues could be mitigated by using fast phase-only SLMs adapted from DMD technology [6].

Although displaying patterns is fast, solving for the correct DMD pattern to display for some desired projector pattern can be computationally expensive. Every iteration of the GS algorithm requires two Fourier transform operations. We run GS for 10 iterations, requiring a total of 18 seconds per pattern on our Intel i7-9700k CPU. Given that every light curtain uses 256 projector patterns, computing a single curtain currently requires 77 minutes. However, more specialized hardware like a GPU or FPGA should speed up our implementation. It may also be possible to recover light curtains of sufficient quality with fewer iterations of GS or by using a more efficient reconstruction algorithm.

8. Societal Impacts

The light curtain system is designed to selectively measure specific 3D regions, and not the entire field of view. While this has positive implications for privacy, a duplicitous entity could use it for optical censorship. Such a system could also project "disguised" inappropriate content that is only legible from a rolling-shutter camera in the right optical configuration. In addition, light curtains are useful for inspection and safety in factories and infrastructure. While this can reduce cost and save lives, it may automate jobs humans currently perform.

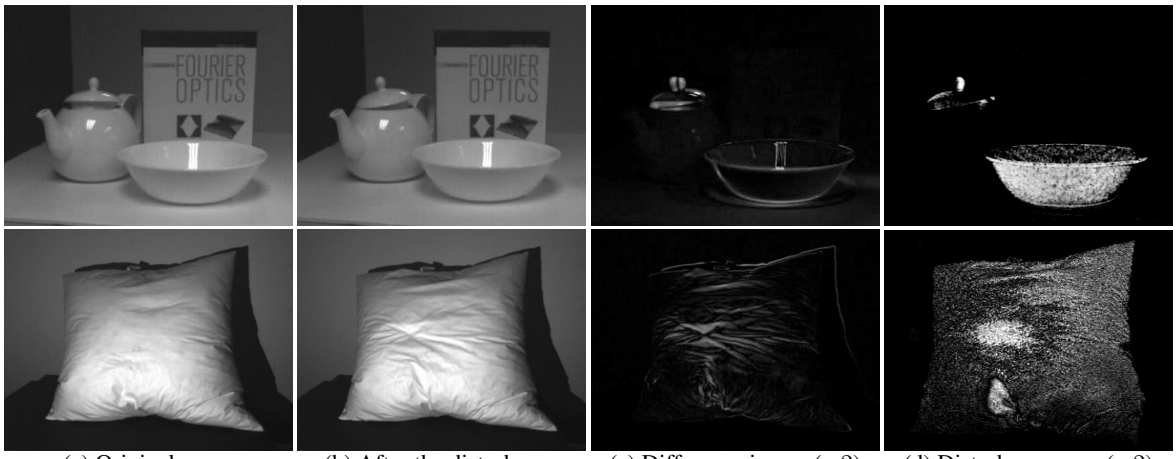

(a) Original scene (b) After the disturbance (c) Difference image (×2) (d) Disturbance map (×2)

Figure 11. Our system can optically detect if objects have been disturbed in a scene. In regions where little texture is present or the pixels are saturated or underexposed, a difference image provides low-intensity, sparse information on whether a scene is disturbed. However, a light curtain more accurately registers any change in surface geometry.

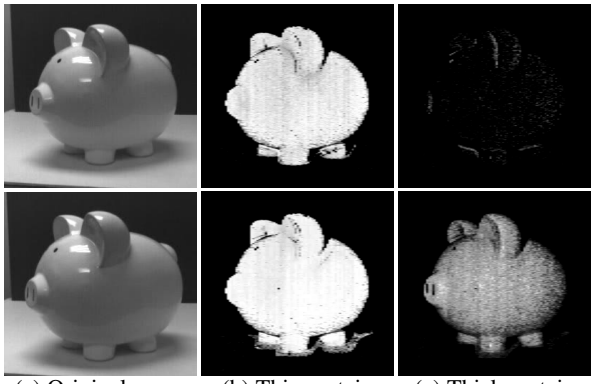

(a) Original scene (b) Thin curtain (c) Thick curtain

Figure 12. Our system can optically detect the magnitude of a disturbance by multiplexing light curtains of different thicknesses. In this diagram, we show a thin curtain and a thick curtain illuminating the scene. **Row 1:** When the disturbance is small, while the thin curtain readily registers the disturbance, the thick curtain receives little signal. **Row 2:** In contrast, when the disturbance is large, both curtains easily detect the disturbance.

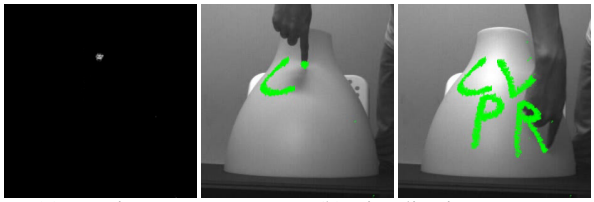

(a) Raw input (b) Visualization

Figure 13. Creating a 3D touch interface with our system. We form a light curtain about 2 cm off the surface of the object, which we can use to detect interactions with the object. By accumulating interactions over time, we can transform any object into a virtual drawing surface.

9. Conclusion and Future Work

In this work, we demonstrated a binary holographic approach for structured lighting in the context of triangulation light curtains. Such a device based on a DMD is fast and light efficient enough to generate light curtains of arbitrary shape when combined with a rolling-shutter camera. We showed that such a system can be used to multiplex multiple curtains into a single image, optically detect disturbances and their magnitudes, and generate three dimensional touch interfaces. All of these applications are enabled by a single easily-calibrated optical configuration.

We implemented the programmability at the illumination end, while retaining the rolling-shutter camera. It is also entirely possible to encode progammability at the sensor end (*e.g.*, by controlling the exposure of individual pixels [36]), while retaining the galvo-scanned laser line at the illumination side. Such an approach could offer certain advantages over binary holography, such as additional light efficiency or improved image quality. However, this requires a more complicated optical setup or fabricating custom sensors.

There are a number of directions for future work. The holographic projector as presented in this paper can be further improved—either with superior hardware like a fast phase SLM [6], better calibration of the forward model by using a camera-in-the-loop approach [23], or more sophisticated reconstruction algorithms than the binary Gerchberg-Saxton presented in Sec. 4.2. Moreover, our holographic projector can most likely be easily applied for other computer vision problems, including real-time epipolar and non-epipolar imaging [20] and structured light 3D sensing under bright sunlight [14].

Acknowledgements. We thank Oliver Kroemer for providing access to the robot arm, and Mark Sheinin for feedback. This work was supported by NSF Grant IIS-1900821.

References

[1] The complete guide to 3d scanners using laser triangulation. https://www.3dnatives.com/en/3d-scanner-laser-triangulation080920174-99/, 2017. 2

[2] Keyence Corporation of America. https://www.keyence.com/products/safety/light-curtain/, 2021. 1, 3

[3] Siddharth Ancha, Gaurav Pathak, Srinivasa G Narasimhan, and David Held. Active safety envelopes using light curtains with probabilistic guarantees. *arXiv preprint arXiv:2107.04000*, 2021. 2

[4] Siddharth Ancha, Yaadhav Raaj, Peiyun Hu, Srinivasa G Narasimhan, and David Held. Active perception using light curtains for autonomous driving. In *European Conference on Computer Vision*, pages 751–766. Springer, 2020. 2

[5] Joseph R Bartels, Jian Wang, William Whittaker, Srinivasa G Narasimhan, et al. Agile depth sensing using triangulation light curtains. In *ICCV*, pages 7900–7908, 2019. 1, 2, 3, 6

[6] Terry A Bartlett, William C McDonald, and James N Hall. Adapting texas instruments dlp technology to demonstrate a phase spatial light modulator. In *Emerging Digital Micromirror Device Based Systems and Applications XI*, volume 10932, page 109320S. International Society for Optics and Photonics, 2019. 4, 7, 8

[7] BR Brown and AW Lohmann. Computer-generated binary holograms. *IBM Journal of research and Development*, 13(2):160–168, 1969. 3

[8] Bryon R Brown and Adolf W Lohmann. Complex spatial filtering with binary masks. *Applied optics*, 5(6):967–969, 1966. 3

[9] Jiyi Cheng, Chenglin Gu, Dapeng Zhang, and Shih-Chi Chen. High-speed femtosecond laser beam shaping based on binary holography using a digital micromirror device. *Optics letters*, 40(21):4875–4878, 2015. 3

[10] Jiyi Cheng, Chenglin Gu, Dapeng Zhang, Dien Wang, and Shih-Chi Chen. Ultrafast axial scanning for two-photon microscopy via a digital micromirror device and binary holography. *Optics letters*, 41(7):1451–1454, 2016. 3

[11] Qiang Geng, Dien Wang, Pengfei Chen, and Shih-Chi Chen. Ultrafast multi-focus 3-d nano-fabrication based on two-photon polymerization. *Nature communications*, 10(1):1–7, 2019. 3

[12] R. W. Gerchberg and W. O. Saxton. A practical algorithm for the determination of phase from image and diffraction plane pictures. *Optik*, 35:237–246, 1972. 5

[13] Mohit Gupta, Amit Agrawal, Ashok Veeraraghavan, and Srinivasa G Narasimhan. Structured light 3d scanning in the presence of global illumination. In *CVPR 2011*, pages 713–720. IEEE, 2011. 2

[14] Mohit Gupta, Qi Yin, and Shree K Nayar. Structured light in sunlight. In *Proceedings of the IEEE International Conference on Computer Vision*, pages 545–552, 2013. 2, 3, 8

[15] Sven TS Holmström, Utku Baran, and Hakan Urey. Mems laser scanners: a review. *Journal of Microelectromechanical Systems*, 23(2):259–275, 2014. 2

[16] Jung-Ping Liu, Ming-Hsuan Wu, and Peter WM Tsang. 3d display by binary computer-generated holograms with localized random down-sampling and adaptive intensity accumulation. *Optics Express*, 28(17):24526–24537, 2020. 3

[17] Kazunobu Masuda, Yusuke Saita, Ryusuke Toritani, Peng Xia, Kouichi Nitta, and Osamu Matoba. Improvement of image quality of 3d display by using optimized binary phase modulation and intensity accumulation. *Journal of Display Technology*, 12(5):472–477, 2016. 5

[18] Kevin J Mitchell, Sergey Turtaev, Miles J Padgett, Tomáš Čižmár, and David B Phillips. High-speed spatial control of the intensity, phase and polarisation of vector beams using a digital micro-mirror device. *Optics express*, 24(25):29269–29282, 2016. 3

[19] Shree K Nayar, Gurunandan Krishnan, Michael D Grossberg, and Ramesh Raskar. Fast separation of direct and global components of a scene using high frequency illumination. In *ACM SIGGRAPH 2006 Papers*, pages 935–944. Association for Computing Machinery, 2006. 2

[20] Matthew O'Toole, Supreeth Achar, Srinivasa G Narasimhan, and Kiriakos N Kutulakos. Homogeneous codes for energy-efficient illumination and imaging. *ACM TOG*, 34(4):1–13, 2015. 2, 3, 8

[21] Matthew O'Toole, John Mather, and Kiriakos N Kutulakos. 3d shape and indirect appearance by structured light transport. In *CVPR*, pages 3246–3253, 2014. 2

[22] Matthew O'Toole, Ramesh Raskar, and Kiriakos N Kutulakos. Primal-dual coding to probe light transport. *ACM TOG*, 31(4):39–1, 2012. 2, 3

[23] Yifan Peng, Suyeon Choi, Nitish Padmanaban, and Gordon Wetzstein. Neural holography with camera-in-the-loop training. *ACM Transactions on Graphics (TOG)*, 39(6):1–14, 2020. 8

[24] Rafael Piestun, Boris Spektor, and Joseph Shamir. On-axis binary-amplitude computer generated holograms. *Optics communications*, 136(1-2):85–92, 1997. 5

[25] Paolo Pozzi, Dean Wilding, Oleg Soloviev, Hans Verstraete, Laurens Bliek, Gleb Vdovin, and Michel Verhaegen. High speed wavefront sensorless aberration correction in digital micromirror based confocal microscopy. *Optics Express*, 25(2):949–959, 2017. 3, 6

[26] Yaadhav Raaj, Siddharth Ancha, Robert Tamburo, David Held, and Srinivasa G Narasimhan. Exploiting & refining depth distributions with triangulation light curtains. In *Proceedings of the IEEE/CVF Conference on Computer Vision and Pattern Recognition*, pages 7434–7442, 2021. 2

[27] Joaquim Salvi, Sergio Fernandez, Tomislav Pribanic, and Xavier Llado. A state of the art in structured light patterns for surface profilometry. *Pattern recognition*, 43(8):2666–2680, 2010. 2

[28] Yoav Y Schechner, Shree K Nayar, and Peter N Belhumeur. Multiplexing for optimal lighting. *IEEE Transactions on pattern analysis and machine intelligence*, 29(8):1339–1354, 2007. 2

[29] Tal Simchony, Rama Chellappa, and Min Shao. Direct analytical methods for solving poisson equations in computer vision problems. *IEEE transactions on pattern analysis and machine intelligence*, 12(5):435–446, 1990. 5

[30] Dustin Stuart, Oliver Barter, and Axel Kuhn. Fast algorithms for generating binary holograms. *arXiv preprint arXiv:1409.1841*, 2014. 3, 5

[31] Dustin Stuart and Axel Kuhn. Single-atom trapping and transport in dmd-controlled optical tweezers. *New Journal of Physics*, 20(2):023013, 2018. 3

[32] Mayuka Tsuji, Hiroyuki Kubo, Suren Jayasuriya, Takuya Funatomi, and Yasuhiro Mukaigawa. Touch sensing for a projected screen using slope disparity gating. *IEEE Access*, 9:106005–106013, 2021. 2, 3, 7

[33] Sergey Turtaev, Ivo T Leite, Kevin J Mitchell, Miles J Padgett, David B Phillips, and Tomáš Čižmár. Comparison of nematic liquid-crystal and dmd based spatial light modulation in complex photonics. *Optics express*, 25(24):29874–29884, 2017. 3, 5

[34] Tomoki Ueda, Hiroyuki Kubo, Suren Jayasuriya, Takuya Funatomi, and Yasuhiro Mukaigawa. Slope disparity gating using a synchronized projector-camera system. In *2019 IEEE International Conference on Computational Photography (ICCP)*, pages 1–9. IEEE, 2019. 2, 3, 6

[35] Jian Wang, Joseph Bartels, William Whittaker, Aswin C Sankaranarayanan, and Srinivasa G Narasimhan. Programmable triangulation light curtains. In *ECCV*, pages 19–34, 2018. 1, 2, 3, 6

[36] Mian Wei, Navid Sarhangnejad, Zhengfan Xia, Nikita Gusev, Nikola Katic, Roman Genov, and Kiriakos N Kutulakos. Coded two-bucket cameras for computer vision. In *Proceedings of the European Conference on Computer Vision (ECCV)*, pages 54–71, 2018. 8